Published in final edited form as:
Cancer Lett. 2010 September 1; 295(1): 69–84. doi:10.1016/j.canlet.2010.02.015.

MUC4 down-regulation reverses chemoresistance of pancreatic cancer stem/progenitor cells and their progenies

Murielle Mimeault[a], **Sonny L. Johansson**[b], **Shantibhusan Senapati**[a], **Navneet Momi**[a], **Subhankar Chakraborty**[a], and **Surinder K. Batra**[a,b,*]

[a]Department of Biochemistry and Molecular Biology, University of Nebraska Medical Center, Omaha, NE 68198-5870, USA

[b]Department of Pathology and Microbiology, University of Nebraska Medical Center, Omaha, NE 68198-5870, USA

Abstract

The present study was undertaken to estimate the therapeutic benefit to down-regulate the MUC4 mucin for reversing chemoresistance of pancreatic cancer (PC) stem/progenitor cells and their progenies. The results have revealed that MUC4 mucin is overexpressed in $CD133^+$ and $CD133^-$ pancreatic cells (PCs) detected in patient's adenocarcinoma tissues while no significant expression was seen in normal pancreatic tissues. The gain- and loss-of-function analyses have indicated that the overexpression of MUC4 in PC lines is associated with a higher resistance to the anti-proliferative, anti-invasive and apoptotic effects induced by gemcitabine. Importantly, the treatment of the MUC4-overexpressing CD18/HPAF-Src cells with gemcitabine resulted in an enrichment of the side population (SP) cells expressing CD133 while the total PC cells including non-SP cells detected in MUC4 knockdown CD18/HPAF-shMUC4 cells were responsive to the cytotoxic effects induced by gemcitabine. These data suggest that the MUC4 down-regulation may constitute a potential therapeutic strategy for improving the efficacy of gemcitabine to eradicate the total PC cell mass, and thereby preventing disease relapse.

Keywords

Pancreatic cancer; Pancreatic stem/progenitor cells; Side population; MUC4 mucin; Chemoresistance; Gemcitabine; Cancer therapies

1. Introduction

The mucin family comprises the secreted and membrane-bound forms of proteins with a high-molecular weight and heavy O-glycosylation sites that participate in the lubrification of luminal epithelial surfaces and protection against external insults [1–3]. Among them, membrane mucin 4 (MUC4), which is constituted by the extracellular and transmembrane domains, and a short cytoplasmic carboxyl-tail, has inspired great interest following the demonstration that it can mediate intracellular signals involved in cancer development [3,4]. A growing body of

*Corresponding author. Address: Department of Biochemistry and Molecular Biology, Eppley Institute for Research in Cancer and Allied Diseases, University of Nebraska Medical Center, Omaha, NE 68198-5870, USA. Tel.: +1 402 559 5455; fax: +1 402 559 6650. sbatra@unmc.edu (S.K. Batra).

Conflict of interest statement
Authors declare no conflict of interest.

experimental evidence has revealed that the enhanced expression of mucins, including MUC4, frequently occurs in cancer cells during disease progression in a large number of aggressive carcinomas such as pancreatic, gastric, non-small cell lung, cervical squamous cell, breast and ovarian cancers [5–12]. MUC4 and other mucins, such as MUC1, can play critical roles for the sustained growth, survival and metastases of cancer cells at distant tissues and organs and drug resistance [3,13–23]. More particularly, we have shown by using both loss- and gain-of-function approaches, a direct association of the aberrant expression of MUC4 mucin with the acquisition of aggressive and metastatic phenotypes of pancreatic cancer (PC) cells [3,15–17,19,24]. Especially, MUC4 overexpression was significantly associated with an enhanced growth rate, motility, invasive and anti-adhesive properties of PC cells *in vitro* and *in vivo* [3,15–17,19,24].

Numerous studies have also revealed that the functional role of the MUC4 oncoprotein in the tumorigenicity and metastases of human pancreatic, colorectal, gallbladder, non-small cell lung, breast and ovarian cancer cells may be mediated, at least in part, *via* a direct physical interaction of MUC4 with the extracellular epidermal growth factor (EGF)-like domain of erbB2 (also designated as HER2/Neu) [8,14,16,18,20,25–27]. This molecular event may lead to a decreased cellular internalization and enhanced phosphorylation of erbB2 receptor tyrosine kinase and activation of the downstream tumorigenic cascades such as mitogen-activated protein kinases (MAPKs) and/ or phosphatidylinostol 3-kinase (PI_3K)/Akt pathways in a cancer cell type-dependent manner [20,25–27]. Importantly, the results from recent studies have also indicated that the MUC4 expression may contribute to the resistance of cancer cells to the cytotoxic effects induced by serum-starvation and chemotherapeutic drugs, *via* erbB2-dependent and -independent mechanisms [22,28]. Hence, all these structural and functional attributes of MUC4 support the potential therapeutic interest in targeting it to prevent cancer progression and improve the current chemotherapeutic regimen options.

In considering these recent works, it appears important to further investigate the implication of the MUC4 oncoprotein in the intrinsic and/or acquired resistance of PC cells to the current treatments and therapeutic interest of its down-regulation for reversing chemoresistance. Therefore, gain- and loss-of-function studies were undertaken to establish the MUC4 functions in the resistance of PC cells to the anti-proliferative, anti-invasive and apoptotic effects induced by chemotherapeutic drug, gemcitabine which is used as the standard of care for treating patients with aggressive and metastatic pancreatic ductal adenocarcinomas. Of particular interest, we also investigated the therapeutic benefit of down-regulating the MUC4 oncoprotein for overcoming the resistance of PC cells to gemcitabine and improving its anti-carcinogenic effects on side population (SP) and non-SP cell fractions detected in the tumorigenic and metastatic CD18/HPAF cell line by fluorescence-activated cell sorting (FACS).

2. Materials and methods

2.1. Materials

Human pancreatic epithelial cell lines, Panc-1 and Mia-PaCa-2 established from primary pancreatic adenocarcinoma and metastatic HPAF-II cells were originally purchased from American Type Culture Collection (Manassas, VA). The stable clones of MUC4 transfected Panc-1 and MiaPaCa-2 cells overexpressing functional MUC4 protein (Panc-1- and MiaPaCa-2-MUC4) and empty-vector transfected Panc-1 and MiaPaCa-2 cell lines (Panc-1- and Mia-PaCa-2-pSectag C) were established as previously described [16,19]. The stable clones of CD18/HPAF cells, in which MUC4 was stably down-regulated by small hairpin RNA (CD18/HPAF-shMUC4), and empty-vector transfected CD18/HPAF-Src cells expressing endogenous MUC4 used as control were prepared as previously described [15]. All PC cells were maintained routinely in Dulbecco's Modified Eagle Medium (DMEM) supplemented with 10% fetal bovine serum (FBS) and antibiotics (100 μg/ml penicillin–streptomycin) in a

37 °C incubator supplied with 5% CO_2. Furthermore, the SP and non-SP cell fractions isolated from PC cell lines by FACS were maintained in keratinocyte serum-free medium (SFM) supplemented with 1% L-glutamine, antibiotics, EGF (10 ng/ml) and fibroblast growth factor (FGF) at 8 ng/ml in a 37 °C incubator supplied with 5% CO_2. DMEM and keratinocyte-SFM and all other culture materials were from Life Technologies (Carlsbad, CA). Dihexyloxacarbocyanine iodide ($DiOC_6(3)$), (3-(4,5-dimethylthiazol-2-yl)-2,5-diphenyltetrazolium bromide (MTT) and EGF were purchased from Sigma–Aldrich (St. Louis, MO), and the broad caspase inhibitor, N-benzyl-oxycarbonyl-Val-Ala-Asp-fluoromethylketone (Z-VAD-FMK) from Calbiochem Corp (San Diego, CA). Gemcitabine was obtained from Eli Lilly and Co. (Indianapolis). The rabbit polyclonal anti-CD133 antibody (H-284) and anti-ABCG2 antibody (B-25), and mouse monoclonal anti-CD44 (HCAM, F-4) antibody and anti-cytochrome *c* (6H2) antibody were purchased from Santa Cruz Biotechnology, Inc. The mouse monoclonal anti-β-actin antibody (clone AC-15) was provided by Sigma–Aldrich (St-Louis, MO, USA) while the mouse monoclonal anti-MUC4 antibody (8G7) was generated in our laboratory [29]. Moreover, rabbit polyclonal antibody directed against the cleaved fragment of caspase-3 or caspase-9 (D330) were purchased from Cell Signaling Technology and rabbit polyclonal antibody recognizing the cleaved human poly (ADP-ribose) polymerase, PARP(197–214) fragment from Calbiochem, Inc (San Diego, CA, USA). The fluorescein isothiocyanate (FITC)-conjugated monoclonal anti-MUC4 antibody was prepared as previously described [29]. The amounts of proteins were estimated by using a detergent-compatible protein assay kit from Bio-Rad Laboratories, Inc. (Hercules, CA).

2.2. Immunohistochemical and double-immunohistofluorescence analyses

Immunohistochemical studies on the localization of MUC4 in non-malignant and malignant patient's pancreatic tissues were done as described previously [5,30,31]. Briefly, the immunostaining was carried out on tissue microarray sections from 66 cases of patients with primary pancreatic adenocarcinomas and ten normal pancreatic tissue cases (US Biomax, Inc., Rockville, MD). Sections were deparaffinized with EZ-DeWax (BioGenex, San Ramon, CA) and rehydrated using graded ethanol solutions. After washing the slides three times with PBS for 5 min, tissue sections were submerged in microwave antigen retrieval solution consisting of 0.01 mol/L citrate buffer (pH 6.0) and subjected to microwave irradiation three times for 3 min. The non-specific immunostaining was blocked using diluted Vectastain normal horse serum (Vector avidin–biotin complex method kit) for 10 min, and the slides were then incubated with primary anti-MUC4 antibody in a humidified chamber for 1 h at room temperature. After washing with PBS, the slides were incubated with biotinylated universal secondary antibody for 30 min and re-washed with PBS. Endogenous peroxidase activity was quenched using 0.3% hydrogen peroxide in methanol/PBS (1:1) for 10 min. After an additional wash, the slides were incubated with avidin–biotin complex method Vectastain solution for 30 min. The tissue sections were submerged in a staining solution containing 3,3′-diaminobenzidine substrate as indicated in the manufacturer's instructions and rinsed three times in water. A reddish brown color precipitate observed on tissue sections indicates a positive immunoreactivity with the tested primary anti-MUC4 antibody. The slides were counterstained with hematoxylin, dehydrated, and permanently mounted with Vecta-Mount permanent mounting medium (Vector Laboratories). Images, which were captured on a Nikon Eclipse E400 microscope (Nikon Corp., Tokyo, Japan) at different magnifications, are representative of analyzed samples. For each tissue section, the intensity of immunoreactivity for each tested signaling elements was semi-quantitatively graded by a surgical pathologist (S.L.J.) on a 0 to +3 scale (0 = no staining, 1+ = week staining, 2+ = moderately strong, and 3 + = strong staining).

In addition, the double-immunohistofluorescence analyses of the co-localization of stem cell-like marker, CD133 antigen (prominin-1) with MUC4 mucin were carried out on

deparaffinized and rehydrated non-malignant and malignant human pancreatic tissue specimens from the patients obtained from UNMC's tissue bank. The tissue slides were blocked in the presence of 10% goat serum for 30 min followed by incubation with the phycoerythrin-conjugated anti-CD133 antibody plus FITC-conjugated anti-MUC4 antibody for 2 h. The slides were washed twice with PBS and processed for immunofluorescent detection as described below for the confocal microscopic analyses of fixed cells.

2.3. Immunoblot analyses

All PC cells were maintained in medium containing 10% FBS and cell lysates were prepared as previously described [29]. The protein concentrations were estimated using a Bio-Rad protein assay kit. For MUC4, the samples corresponding to 20 μg proteins were resolved by electrophoresis on a 2% SDS-agarose gel under reducing conditions [29]. For immunoblot analyses of cytosolic cytochrome *c*, cleaved caspase-9 or −3 and PARP fragment, the samples were resolved on a 15% SDS–polyacrylamide gel under reducing conditions. For β-actin used as internal control, the samples were resolved on a 10% SDS–polyacrylamide gel under similar conditions. The proteins were transferred onto an immobilon-P transfer membrane and blocked in 5% non-fat dry milk in PBS for 2 h and subjected to the standard immunodetection procedure. At the end of incubation, the blot was washed in TBST (50 mM Tris–HCl, pH 7.4, 150 mM NaCl and 0.05% Tween) and incubated with horseradish peroxidase-conjugated secondary antibody (Amersham Biosciences, Piscataway, NJ) for 1 h. Antibody–antigen complexes were visualized using enhanced chemiluminescence kit (Amersham Biosciences).

2.4. Confocal microscopy analyses

All PC cells were grown at a low density on sterilized cover slips for 24 h, washed with phosphate buffered saline (PBS), and fixed in ice-cold methanol at −20 °C for 2 min [30–32]. The non-specific immunostaining was blocked using 10% goat serum for 30 min, and the cells were incubated with monoclonal FITC-conjugated anti-MUC4 antibody diluted in PBS for 1 h at room temperature. After three washes with PBS, nuclei were counterstained with 4′, 6-diamidino-2-phenylindole (DAPI) and mounted on glass slides in anti-fade Vectashield mounting medium (Vector Laboratories, Burlingame, CA). Immunofluorescence staining was observed under a confocal laser scanning microscope (LSM 410, Zeiss, Gottingen, Germany).

2.5. Cell culture and growth assays

All tested PC cell lines were maintained in complete DMEM culture medium. For growth assays, the cells were seeded on 96-well plates at a density of 3×10^4 cells/well in a total volume of 200 μl culture medium. After three days, the cell growth assays were performed in DMEM medium containing 1% FBS as mentioned previously [30–33]. Gemcitabine at different concentrations of 10– 200 nM was also added to the culture medium. After incubation for 48 h, the rate of cell growth was estimated by a MTT colorimetric test [34].

2.6. In vitro invasion assays

The invasive potential of PC cells was estimated by their ability to penetrate a Matrigel-invasion chamber with a Falcon cell culture insert 8 μm pore size PET membrane, with a thin layer of matrigel matrix acting as a basement membrane *in vivo*, and allowing an estimate of the metastatic potential of tumor cells *in vitro* [15,19,30,33]. PC cells were untreated (control) or pretreated with 50 nM gemcitabine for 24 h, and during cell invasion assay for an additional 24 h. For each experiment, 1×10^5 PC cells/well in a total volume of 2 ml serum-free medium without gemcitabine (control) or containing gemcitabine were loaded into the top of the BD BioCoat Matrigel cell invasion chamber according to the manufacturer's instructions. At the end of incubation, the invasive cells reaching the lower chamber were stained with a Diff-Quick stain set and counted in different fields at a magnification of × 100 using a

hemocytometer by phase-contrast microscopy. The results are presented as the average number of invasive cells per representative field.

2.7. Flow cytofluorometric analyses

All PC cells were grown at a density of 5×10^5 cells on 25 cm^2 dishes as previously described and treated with different concentrations of gemcitabine, in the absence or presence of broad caspase inhibitor, Z-VAD-FMK. In all experiments, the cells were kept at a sub-confluent level to avoid contact inhibition. More specifically, in order to determine the influence of gemcitabine treatment on the cellular cycle progression of CD18/HPAF-Src and CD18/ HPAF-shMUC4 cells, the cytometric analyses by FACS were performed 48 h after the addition of different concentrations of gemcitabine. Moreover, the apoptotic effect induced by gemcitabine on tested PC cells was estimated by FACS analyses after four days of drug treatment initiation. The concentrations of 1–10 μM gemcitabine inducing a significant apoptotic effect, were used in these experiments. The DNA content estimation of each sample was performed after staining with the propidium iodide by FACS™ analyses essentially as previously described [30–33].

2.8. Estimation of mitochondrial transmembrane potential and cytosolic cytochrome c release

To determine whether the apoptotic effect induced by gemcitabine in CD18/HPAF-Src and CD18/HPAF-shMUC4 cells is mediated *via* a mitochondrial pathway, the mitochondrial membrane potential (MMP) and the amount of cytosolic cytochrome c were estimated as previously described [30–33,35]. For MMP analyses, PC cells were untreated (control) or treated with 1–10 μM gemcitabine for four days. The adherent and floating cells were collected by centrifugation and washed in PBS. The pellets corresponding to approximately 1×10^6 cells were resuspended in 1 ml PBS containing the cationic, lipophilic and fluorescent dye, 40 nM $DiOC_6(3)$, which specifically accumulates within the mitochondrial compartment in a MMP-dependent manner [35]. After incubation at 37 °C for 20 min, the accumulation of $DiOC_6(3)$ within the mitochondria of cells was measured by FACS analyses. Moreover, the amounts of cytochrome *c* present in the cytosolic extracts of each sample were estimated following the method described in the ELISA kit from Calbiochem Inc. with a human anti-cytochrome *c* antibody [30–33,36]. In addition, the cytochrome *c* in cytosolic extracts obtained after treatment of PC cells with 10 μM gemcitabine were also analyzed by 15% SDS–polyacrylamide gel electrophoresis and immunoblotting as above described by using mouse monoclonal anti-cytochrome *c* antibody (6H2, sc-13561; Santa Cruz Biotechnology).

2.9. Isolation of the SP and non-SP cell fractions from the human CD18/HPAF cell line by flow cytometry and colony-forming assays

The CD18/HPAF cell line (1×10^6 cells/ml) were stained with Hoechst buffer containing a final concentration of 2 μg/ml fluorescent Hoechst at 37 °C for two hours in the absence or presence of an ABC transporter inhibitor, 50 μM verapamil and the small subpopulations of SP and non-SP cells were isolated by fluorescence-activated cell sorting (FACS) as previously described [32,37]. The analyses and sorting of the viable SP and non-SP cell fractions were done using a FACS Aria flow cytometer with a DIVA software (Becton Dickinson Biosciences, San Jose, CA). The SP and non-SP cell fractions were collected after FACS and the expression level of the CD133 marker, without apparent further phenotypic and differentiation changes in these two cultured cell subpopulations, was obtained by maintaining the cells in serum-free keratinocyte culture medium containing exogenous EGF plus FGF before their use.

The monolayer clonogenic assays were then performed to estimate the self-renewal capacity of SP and non-SP cell fractions isolated from the HPAF/CD18 cell lines by FACS. For each assay, 500 viable SP or non-SP cells obtained after cell sorting were suspended in keratinocyte

medium onto a 120 mm dish. All samples were plated in triplicate. After 14 days, the cultures were fixed and directly stained with a crystal violet solution and colonies were counted.

2.10. Quantitative real time-polymerase chain reaction analyses

The SP and non-SP cell fractions isolated from the CD18/ HPAF cell line were maintained in serum-free keratinocyte culture medium containing exogenous EGF plus FGF and the expression levels of stem cell-like markers (CD133, CD44 and ABCG2) as well as MUC4 were estimated by quantitative real time-polymerase chain reaction (QRT– PCR). After incubation, the cells were collected by centrifugation, and the total cellular RNA was extracted from cultured cell pellets using the RNeasy kit (Qiagen), according to the manufacturer's instructions [31,38]. Total cellular RNA was reverse-transcribed and QRT–PCR was performed using SYBR Green method. The primer sequences used to estimate the gene expression levels of human signaling products by QRT-PCR were as follows: 5′-3′ for CD133: (forward: CACTTACGGCACTCTTCACCT; reverse: TGCAC-GATG CCACTTTCTCAC); CD44 (forward: TCCATCA AAGGCATTGGGCAG; reverse: AACCTGCCGCTTTGCAGG TGT); ABCG2 (forward: TGGCTGTCATGGCTTCAGTA; reverse: GCCACGTGATTCTTCCACAA); MUC4: (forward: GTGACCATGGAGGCCAGTG; reverse: TCATGCTC AGG TGCTCACAG); and β-actin (forward: TGGACATCCGCAAA-GACCTG; reverse: CCGATCCACACGGAGTACTT).

2.11. Statistical analyses

Statistical analyses were performed using the Student's *t*-test to compare the results with *P* values <0.05 indicating statistically significant differences.

3. Results

3.1. Analyses of the MUC4 expression level and its co-localization with CD133 stem cell-like marker in non-malignant and malignant pancreatic adenocarcinoma tissues

We have analyzed the expression level of MUC4 by immunohistochemistry on a tissue microarray from patients comprising sections from 66 cases of pancreatic adenocarcinomas and 10 normal pancreatic tissue cases. An expression level of MUC4 varying from weak to strong was seen within the cytoplasm and at the plasmic membrane of the malignant epithelial cells in 82.0% cases of PC patients, whereas no expression was observed in the normal pancreas (Fig. 1A and Table 1). Since PC stem/progenitor cells can play a critical role in PC progression and treatment resistance, we have also investigated the expression level of the CD133 stem cell-like marker and its co-localization with MUC4 in non-malignant and malignant pancreatic epithelial cells in pancreatic tissue specimens from patients. The immunoconfocal analyses of the expression of CD133 revealed that this stem cell-like marker is detectable only in a very rare subpopulation of pancreatic epithelial cells in the basal compartment in non-malignant pancreatic tissue specimens (Fig. 1B). In contrast, the CD133 protein was only detected in a small subset of PC cells dispersed through the epithelial compartment in pancreatic adenocarcinoma tissues from patients (Fig. 1B). Importantly, the data of immunoconfocal analyses have also indicated that the MUC4 oncoprotein was expressed at a high level in both the small $CD133^+$ cell subpopulation as well as the bulk tumor mass of the $CD133^-$ PCs in malignant pancreatic tissue specimens from patients while it was not detected in non-malignant pancreatic tissues (Fig. 1B). Particularly, the MUC4 was co-localized with the CD133 stem cell-like marker in the epithelial compartment in a similar small subset of PC cells detected in pancreatic adenocarcinoma tissues.

3.2. Estimation of anti-proliferative and anti-invasive effects induced by gemcitabine treatment on MUC4-expressing and non-expressing-PC cells

The immunoblot and immunoconfocal analyses have revealed that no expression of MUC4 was seen in empty vector-transfected Panc-1- and MiaPaCa-2-pSectag C cells while significant levels of MUC4 were detected and mainly localized to the membrane and cytoplasm in the Panc-1- and MiaCaPa-2-MUC4 stable clones engineered for overexpressing functional MUC4 protein (Fig. 2A and B). Moreover, the immunoblot and immuno-confocal analyses have indicated that MUC4 was expressed at high levels and mainly localized to the membrane and cytoplasm in scrambled CD18/ HPAF-shMUC4 cells expressing endogenous MUC4. In contrast, a weak expression of MUC4 was detected in the CD18/HPAF-shMUC4 stable transfectant pool obtained by down-regulating MUC4 in highly tumorigenic and metastatic CD18/HPAF cells by small hairpin RNA (shRNA) (Fig. 2A and B).

We have investigated the anti-proliferative and anti-invasive effects induced by the current clinical chemotherapeutic drug, gemcitabine on MUC4 expressing and non-expressing-PC cell lines. A range of effective concentrations for gemcitabine that can inhibit the proliferation and invasive ability of PC cells were used. The results from MTT tests and *in vitro* invasion assays have indicated that the Panc-1-MUC4 and Mia-PaCa-2-MUC4 cells engineered for overexpressing MUC4 were less sensitive to the anti-proliferative and anti-invasive effects induced by gemcitabine as compared to MUC4 non-expressing Panc-1-pSectag C and MiaPaCa-2-pSectag C cells (Figs. 3 and 4). The values of the half maximal inhibitory concentration (IC_{50}) obtained for Panc-1-MUC4 (59 ± 4 nM) and MiaPaCa-2-MUC4 cells (75 ± 5 nM) were significantly higher that the values for Panc-1-pSectag C (18 ± 2 nM; $p < 0.0001$) and MiaPaCa-2-pSectag C (35 ± 1 nM; $p < 0.001$), respectively. Moreover, the results from MTT tests and invasion assays have also revealed that the MUC4 down-regulation in CD18/ HPAF-shMUC4 cells, was accompanied by an enhanced sensitivity of PC cells to the growth and invasion inhibitory effects induced by gemcitabine relative to scrambled CD18/HPAF-Src expressing MUC4 (Figs. 3 and 4). Specifically, the IC_{50} value obtained for CD18/HPAF-shMUC4 cells (21 ± 2 nM) was significantly lower than the value for CD18/HPAF-Src (59 ± 5 nM; $p < 0.0001$). Moreover, the FACS analyses of the cell populations in the cell cycle have revealed that the gemcitabine treatment of MUC4-silenced CD18/HPAF-shMUC4 cells during two days resulted in a higher percentage of PC cells in G_1/early S phase in conjunction with a reduction in the number of cells in the S phase relative to empty-vector transfected CD18/ HPAF-Src cells expressing endogenous MUC4 (control) (Fig. 3 and Table 2; $p < 0.0001$). In addition, the data from *in vitro* invasion assays have also indicated that CD18/HPAF-shMUC4 cells displayed a weaker invasive ability and were more sensitive to the anti-invasive effect induced by gemcitabine than scrambled CD18/HPAF-Src cells (Fig. 4; $p < 0.0001$).

3.3. Estimation of apoptotic effects induced by gemcitabine treatment on MUC4-expressing and non-expressing-PC cells

The percentages of apoptotic cell death induced by gemcitabine on PC cells were estimated by the flow cytometric analyses and the apoptotic cell number in the sub-G1 phase was quantified. A range of effective concentrations for gemcitabine that can trigger apoptotic death in PC cells were used. As shown in Figs. 5 and 6, the increasing concentrations of gemcitabine induced a higher rate of apoptotic death on MUC4 negative Panc-1- and MiaPaCa-2-pSectag C cells than on Panc-1-MUC4 and Mia-PaCa-2-MUC4 cells engineered for overexpressing MUC4. More specifically, 10 μM gemcitabine caused a higher rate of the apoptotic death in MUC4 non-expressing Panc-1-pSectag C (68.2 ± 4.4%) and MiaPaCa-2-pSectag C cells (64.1 ± 4.2%) as compared to Panc-1-MUC4 (32.2 ± 4.1%; $p < 0.0001$) and MiaPaCa-2-MUC4 (31.4 ± 3.0%; $p < 0.0001$) cells, respectively. Furthermore, the results of the FACS analyses have also indicated that the gemcitabine treatment of the empty-vector transfected CD18/ HPAF-Src cells induced, in a concentration-dependent manner, an increase in the apoptotic cell population

as compared to untreated PC cells (control) after four days of treatment (Figs. 5 and 6). Importantly, the MUC4-silenced CD18/HPAF-shMUC4 cells were, however, more responsive to the apoptotic effects induced by gemcitabine than scrambled CD18/HPAF-Src cells expressing high levels of endogenous MUC4 used as control (Figs. 5 and 6). More specifically, 10 μM gemcitabine induced a higher rate of apoptosis in CD18/HPAF-shMUC4 (63.8 ± 3.4%) as compared to CD18/HPAF-Src cells (42.6 ± 4.0%, $p < 0.0001$) (Fig. 6).

3.4. Establishment of the role of the caspase pathway in the apoptotic effect induced by gemcitabine on CD18/HPAF cells

To assess whether the cytotoxic effects induced by gemcitabine is mediated through a mitochondrial pathway-dependent caspase activation, an estimation of the effects of gemcitabine treatment on the mitochondrial transmembrane potential (MMP) and cytosolic cytochrome *c* was performed by FACS analyses and ELISA assays on the scrambled CD18/HPAF-Src cells overexpressing MUC4 and MUC4-silenced CD18/ HPAF-shMUC4 cells. As shown in Fig. 7A and B, the continuous treatment of the PC cells for four days with 1–10 μM gemcitabine was accompanied by a decrease of MMP, as indicated by the shoulder of the peak and enhanced percentages of depolarized cells as well as an increase of cytochrome c amount released in cytosol as compared to the stained PC cells that were untreated (control). The gemcitabine treatment of the MUC4-silenced CD18/HPAF-shMUC4 was, however, accompanied by a higher mitochondrial membrane depolarizing effect and percentage of depolarized cells as well as cytosolic cytochrome c amount as compared to scrambled CD18/HPAF-Src overexpressing MUC4 (Fig. 7A – C). More specifically, the data of percentage of depolarized cells and cytosolic cytochrome *c* amount induced by 10 μM gemcitabine treatment on the MUC4-silenced CD18/HPAF-shMUC4 (58.4 ± 1.3% and 21.0 ± 1.9 ng/ml) were significantly more elevated as compared to the values obtained for scrambled CD18/HPAF-Src cells (41.7 ± 4.0% and 14.7 ± 0.7 ng/ml; $p < 0.0001$), respectively.

Consistent with the implication of the activation of caspase pathway in apoptotic cell death, the results from Western blot analyses have also indicated that the MUC4-silenced CD18/HPAF-shMUC4 treated with 10 μM gemcitabine showed more cytosolic cytochrome c amount and cleaved caspases-9 and −3 and PARP fragments than the scrambled CD18/HPAF-Src cells (Fig. 7D). Moreover, the results from FACS analyses have also revealed that the broad spectrum caspase inhibitor, Z-VAD-FMK at 50 μM markedly abrogated the percentage of apoptotic cells induced by gemcitabine on all tested PC cell lines including CD18/HPAF-Src and -shMUC4 cells (Fig. 6).

3.5. Characterization of the SP and non-SP cell fractions isolated from the CD18/HPAF cell line and the estimation of cytotoxic effects induced by MUC4 down-regulation and gemcitabine treatment

The results from the FACS analyses have indicated the presence of a small side population (SP) cell fraction representing about 0.9% of the total cell mass in the highly tumorigenic and metastatic CD18/ HPAF pancreatic cell line (Fig. 8A). The SP cell fraction was significantly reduced in the presence of the ABC transporter inhibitor, 50 μM verapamil. These data suggest that the SP phenotype may be associated with a high expression of ABC multidrug efflux pumps, including ABCG2, in these immature cells as previously reported for numerous cancer stem/progenitor cell types [37,39,40]. We have successfully isolated the SP and non-SP cell fractions from the parental CD18/HPAF cell line by FAC sorting and maintained these cells in serum-free culture medium. As shown in Fig. 8, the small SP cell subpopulation possesses a greater self-renewal ability and expresses higher levels of stem cell-like markers, including CD133, CD44 and ABCG2 drug transporter than the non-SP cell fraction ($p < 0.0001$). Interestingly, the SP and non-SP cell fractions isolated from the CD18/HPAF cell line, also express significant levels of the MUC4 oncoprotein (Fig. 8C and D).

Importantly, the results from FACS analyses revealed that the treatment of parental CD18/HPAF or empty-vector CD18/HPAF-Src cells with 5 μM gemcitabine for four days was accompanied by a significant increase in the percentage of viable SP cells while the number of cells in the bulk PC cell mass including non-SP cells was reduced as compared to nontreated cells used as control (Fig. 8E). The continued treatment of CD18/HPAF-Src cells with 5 μM gemcitabine for a longer period of seven days resulted in a marked enrichment of viable SP cells while the number of cells detected in bulk PC cell mass including non-SP cells was almost completely eradicated (Fig. 8E). Of therapeutic interest, the gemcitabine treatment of CD18/HPAF-shMUC4 cells was however associated with a significant decrease in the percentage of viable SP as well as the number of cells in the bulk PC cell mass including non-SP cells detected by Hoechst dye exclusion technique (Fig. 8E).

4. Discussion

Numerous studies have revealed that the enhanced expression of mucins, including the MUC4, in epithelial cancer cells during progression from non-neoplastic to locally invasive and metastatic stages may be associated with their acquisition of more aggressive phenotypes and survival advantages and poor prognosis of cancer patients [5–11]. It has been shown that MUC4 overexpression in tumor cells may enhance their malignant behavior and repress apoptosis through different mechanisms including an up-regulation of diverse growth factor and anti-apoptotic pathways, and interference with cell–cell and cell-extracellular matrix (ECM) interactions [3,13–15,17–22]. Thereby, the MUC4 oncoprotein may promote the sustained growth, survival, invasion, local and distant metastases and treatment resistance of cancer cells [3,13–15,17–22]. In this regard, the results of the present study revealed that MUC4 is expressed in a small subset of $CD133^+$ PC cells dispersed through tumors and the bulk mass of $CD133^-$ PC cells in certain cases of PC patients, as compared to non-malignant pancreatic tissues (Fig. 1). This observation is in agreement with some previous studies that indicated that MUC4 was overexpressed in pancreatic adenocarcinoma specimens during disease progression [5–7]. More specifically, we have demonstrated that an increase of the MUC4 expression level occurs in pancreatic ductal adenocarcinomas as compared to normal pancreatic or chronic pancreatitis tissue [5]. Moreover, it has also been reported that small subpopulations of $CD133^+$/ $CXCR4^-$ and $CD133^+$/$CXCR4^+$ PC cells were detected in the bulk tumor mass and the invasive front of PC samples, respectively [41,42]. Hence, MUC4 overexpression in $CD133^+$ PC stem/progenitor cells and their differentiated $CD133^-$ progenies may contribute to their malignant transformation during PC development and disease progression.

In support with the potential implications of MUC4 oncoprotein in enhanced malignant character and treatment resistance of PC cells, the results have also revealed that the ectopic overexpression of MUC4 in Panc-1 and MiaPaCa-2 cells (Panc-1- and MiaPaCa-2-MUC4) was associated with a more aggressive behavior and decreased sensitivity of these PC cells to the cytotoxic effects induced by the current chemotherapeutic drug, gemcitabine relative to MUC4 non-expressing Panc-1 and MiaPaCa-2 cells (Panc-1- and MiaPaCa-2-pSectag C) (Figs. 2–6). These observations are consistent with the data from prior studies indicating that the overexpression of human MUC4 or its rat ortholog, designated as sialomucin complex (SMC), as well as other mucins in cancer cells may be associated with more malignant phenotypes and an enhanced rate of tumor growth and metastases [22,23,43–45]. Moreover, it has been reported that MUC4/SMC-overexpressing cancer cells were more resistant to the cytotoxic effects induced by diverse therapeutic treatments, and displayed a high ability to evade immune surveillance [22,23,43–45]. In particular, the overexpression of the high-molecular weigh glycoprotein, MUC4 on the target tumor cell surface can mask the surface antigens, and thereby decrease their accessibility and the cytotoxic response induced by monoclonal anti-erbB2 antibody, trastuzumab (as known as herceptin) as well as the tumor cell killing mediated by immune cells [43–45]. Furthermore, the ectopic overexpression of

MUC4/SMC in human A375 melanoma cells and MCF7 breast cancer cells has been associated with a loss of cellular adhesion and resistance to apoptosis induced by serum-starvation or cisplatin treatment in these cancer cells *in vitro* [22]. In the same way, human A375 melanoma cells engineered to overexpress MUC4/SMC were more resistant than MUC4 non-expressing melanoma cells to the anti-proliferative effect induced by taxol, doxorubicin, vinblastine, rhodamine-123 or 2-deoxyglucose as well as the apoptotic and/or necrotic response mediated by doxorubicin [21]. Importantly, the induction of MUC4/ SMC overexpression in A375 melanoma cells also resulted in an enhanced tumor cell growth, decreased rate of apoptotic death and a higher incidence of lung metastases as compared to A375 melanoma cells with suppressed expression of MUC4/SMC in a xenograft model *in vivo* [13,14]. Hence, it appears that an up-regulation of MUC4/ SMC expression in cancer cells during cancer progression may represent a transforming event that provides them with an enhanced tumorigenic and metastatic potential and resistance to diverse cytotoxic agents.

Although efforts have been made to improve the diagnosis, surgical treatment and first-line gemcitabine chemotherapies in the care of PC patients, the lack of early diagnostic biomarkers, rapid progression to locally advanced and metastatic PCs and chemoresistance generally lead to disease recurrence and the death of patients about five months after diagnosis and treatment initiation [46–53]. Lack of efficacy of the current chemotherapeutic regimens underlines the urgent need to identify molecular targets to develop new combination therapies for overcoming chemoresistance, side effects at high doses of drugs and disease relapse. In this regard, the results in this study have indicated that MUC4 down-regulation in highly tumorigenic and metastatic CD18/HPAF cells resulting in stable transfectant pool (CD18/HPAF-shMUC4), decreased their aggressive behavior and enhanced their sensitivity to anti-proliferative, anti-invasive and apoptotic effects induced by gemcitabine treatment as compared to scrambled CD18/HPAF-Src cells overexpressing endogenous MUC4 (Figs. 3–6). More specifically, the results have indicated that the gemcitabine was more effective to induce the anti-proliferative effect through a blockade of MUC4-silenced CD18/HPAF-shMUC4 cells in the G_1-early S phases of the cell cycle as compared to scrambled CD18/HPAF-Src cells (Fig. 3 and Table 2). Moreover, the results have revealed that the gemcitabine treatment induced a higher rate of apoptotic cell death in MUC4-silenced CD18/ HPAF-shMUC4 cells as compared to scrambled CD18/ HPAF-Src cells, at least in part, through a up-regulation of depolarization of the mitochondrial membrane, cytochrome *c* release into cytosol, and activation of caspase pathway (Figs. 5–7).

Importantly, recent accumulating lines of experimental evidence have revealed that highly tumorigenic and migrating PC stem/progenitor cells, also designated as PC-initiating cells, may be more resistant to the current chemotherapies, and thereby provide critical functions in tumor recurrence and metastases at distant tissues after treatment initiation and disease relapse [41,54,55]. In support with the critical implication of PC stem/progenitor cells in the chemoresistance, the data from FACS analyses also revealed that the treatment of CD18/ HPAF-Src cells with 5 μM gemcitabine was accompanied by an enrichment of viable SP cells expressing CD133 stem cell-like marker and displaying a high self-renewal potential than the non-SP cell fraction (Fig. 8E). In contrast, the number of cells in the bulk PC cell mass including non-SP cells was reduced as compared to untreated CD18/HPAF-Src cells used as a control (Fig. 8E). It is of great therapeutic interest that although SP cells detected in MUC4-over-expressing CD18/HPAF-Src were not sensitive to a high concentration of 5 μM gemcitabine, the SP fraction from MUC4-knockdown CD18/HPAF-shMUC4 cells was responsive to the cytotoxic effects induced by gemcitabine treatment (Fig. 8E). Altogether, these observations suggest that the MUC4 down-regulation can partially reverse the resistance of $CD133^+$ PC-initiating cells and their differentiated $CD133^-$ progenies to the current chemotherapeutic drug, gemcitabine and thereby improve its cytotoxic effects. These data are consistent with the results from previous studies indicating that the MUC4 oncoprotein may confer more malignant

phenotypes and survival advantages to PC cells and contribute to their chemoresistance through erbB2-dependent and anti-apoptotic pathways [15,16,28]. Moreover, it has been reported that the down-regulation of endogenous MUC4 in the JIMT-1 breast cancer cell line improved the apoptotic effect induced by serum-starvation and the chemotherapeutic drug, cisplatin [22]. In addition, it has been shown that the treatment of PC cells with the current chemotherapeutic drug, gemcitabine led to an enrichment in the number of PC cells with the stem celllike properties *in vitro* and *in vivo* [41,54,55]. More specifically, it has been observed that a small subpopulation of $CD133^+$ PC cells with stem cell-like properties isolated from patient's malignant primary neoplasm was more resistant to gemcitabine than the $CD133^-$ PC cell fraction [41]. It has also been noticed that the $CD133^+$ L3.6pl cells were more resistant to gemcitabine treatment as compared to the $CD133^-$ L3.6pl cells *in vitro* and an enrichment of $CD133^+$ L3.6pl cell fraction in the total tumor cell mass occurred after gemcitabine treatment relative to the control in mice *in vivo* [41]. In the same way, the gemcitabine treatment of pancreatic tumor xenografts *in vivo* also resulted in an enrichment in a subpopulation of PC cells expressing a high level of stem cell-like markers such as aldehyde dehydrogenase (ALDH) and CD24 [54].

Taken together, the results of the present investigation revealed that the MUC4 overexpression in $CD133^+$ PC-initiating cells and their differentiated $CD133^-$ progenies during PC progression may contribute to their aggressive behavior and resistance to the main current chemotherapeutic drug, gemcitabine. Hence, the down-regulation of the MUC4 oncoprotein may represent a promising therapeutic strategy for reversing chemoresistance and eradicating the total PC cell mass. Further *in vivo* studies should allow us to corroborate these *in vitro* data supporting the therapeutic benefit of down-regulating MUC4 mucin to improve the anti-carcinogenic efficacy of gemcitabine-based chemotherapies against locally advanced and metastatic PCs, and thereby prevent disease recurrence and the death of PC patients.

Acknowledgments

We thank the Molecular Biology Core Facility at the University of Nebraska Medical Center for FACS analyses. We thank Ms. Kristi L. Berger for editing the manuscript.

Funding

The authors on this work are supported by grants from the National Institutes of Health (CA78590, CA111294, CA133774 and CA131944).

References

1. Singh PK, Hollingsworth MA. Cell surface-associated mucins in signal transduction. Trends Cell Biol 2006;16:467–476. [PubMed: 16904320]
2. Hattrup CL, Gendler SJ. Structure and function of the cell surface (tethered) mucins. Annu. Rev. Physiol 2008;70:431–457. [PubMed: 17850209]
3. Chaturvedi P, Singh AP, Batra SK. Structure, evolution, and biology of the MUC4 mucin. FASEB J 2008;22:966–981. [PubMed: 18024835]
4. Carraway KL III, Funes M, Workman HC, Sweeney C. Contribution of membrane mucins to tumor progression through modulation of cellular growth signaling pathways. Curr. Top. Dev. Biol 2007;78:1–22. [PubMed: 17338913]
5. Andrianifahanana M, Moniaux N, Schmied BM, Ringel J, Friess H, Hollingsworth MA, Buchler MW, Aubert JP, Batra SK. Mucin (MUC) gene expression in human pancreatic adenocarcinoma and chronic pancreatitis: a potential role of MUC4 as a tumor marker of diagnostic significance. Clin. Cancer Res 2001;7:4033–4040. [PubMed: 11751498]
6. Saitou M, Goto M, Horinouchi M, Tamada S, Nagata K, Hamada T, Osako M, Takao S, Batra SK, Aikou T, Imai K, Yonezawa S. MUC4 expression is a novel prognostic factor in patients with invasive ductal carcinoma of the pancreas. J. Clin. Pathol 2005;58:845–852. [PubMed: 16049287]

7. Nagata K, Horinouchi M, Saitou M, Higashi M, Nomoto M, Goto M, Yonezawa S. Mucin expression profile in pancreatic cancer and the precursor lesions. J. Hepatobiliary Pancreat. Surg 2007;14:243–254. [PubMed: 17520199]
8. Karg A, Dinc ZA, Basok O, Ucvet A. MUC4 expression and its relation to ErbB2 expression, apoptosis, proliferation, differentiation, and tumor stage in non-small cell lung cancer (NSCLC). Pathol. Res. Pract 2006;202:577–583. [PubMed: 16814944]
9. Rakha EA, Boyce RW, bd El-Rehim D, Kurien T, Green AR, Paish EC, Robertson JF, Ellis IO. Expression of mucins (MUC1, MUC2, MUC3, MUC4, MUC5AC and MUC6) and their prognostic significance in human breast cancer. Mod. Pathol 2005;18:1295–1304. [PubMed: 15976813]
10. Chauhan SC, Singh AP, Ruiz F, Johansson SL, Jain M, Smith LM, Moniaux N, Batra SK. Aberrant expression of MUC4 in ovarian carcinoma: diagnostic significance alone and in combination with MUC1 and MUC16 (CA125). Mod. Pathol 2006;19:1386–1394. [PubMed: 16880776]
11. Davidson B, Baekelandt M, Shih I. MUC4 is upregulated in ovarian carcinoma effusions and differentiates carcinoma cells from mesothelial cells. Diagn. Cytopathol 2007;35:756–760. [PubMed: 18008338]
12. Munro EG, Jain M, Oliva E, Kamal N, Lele SM, Lynch MP, Guo L, Fu K, Sharma P, Remmenga S, Growdon WB, Davis JS, Rueda BR, Batra SK. Upregulation of MUC4 in cervical squamous cell carcinoma: pathologic significance. Int. J. Gynecol. Pathol 2009;28:127–133. [PubMed: 19188823]
13. Komatsu M, Tatum L, Altman NH, Carothers Carraway CA, Carraway KL. Potentiation of metastasis by cell surface sialomucin complex (rat MUC4) a multifunctional anti-adhesive glycoprotein. Int. J. Cancer 2000;87:480–486. [PubMed: 10918186]
14. Komatsu M, Jepson S, Arango ME, Carothers Carraway CA, Carraway KL. Muc4/sialomucin complex, an intramembrane modulator of ErbB2/HER2/Neu, potentiates primary tumor growth and suppresses apoptosis in a xenotransplanted tumor. Oncogene 2001;20:461–470. [PubMed: 11313977]
15. Chaturvedi P, Singh AP, Moniaux N, Senapati S, Chakraborty S, Meza JL, Batra SK. MUC4 mucin potentiates pancreatic tumor cell proliferation, survival, and invasive properties and interferes with its interaction to extracellular matrix proteins. Mol. Cancer Res 2007;5:309–320. [PubMed: 17406026]
16. Chaturvedi P, Singh AP, Chakraborty S, Chauhan SC, Bafna S, Meza JL, Singh PK, Hollingsworth MA, Mehta PP, Batra SK. MUC4 mucin interacts with and stabilizes the HER2 oncoprotein in human pancreatic cancer cells. Cancer Res 2008;68:2065–2070. [PubMed: 18381409]
17. Singh AP, Moniaux N, Chauhan SC, Meza JL, Batra SK. Inhibition of MUC4 expression suppresses pancreatic tumor cell growth and metastasis. Cancer Res 2004;64:622–630. [PubMed: 14744777]
18. Singh AP, Chaturvedi P, Batra SK. Emerging roles of MUC4 in cancer: a novel target for diagnosis and therapy. Cancer Res 2007;67:433–436. [PubMed: 17234748]
19. Moniaux N, Chaturvedi P, Varshney GC, Meza JL, Rodriguez-Sierra JF, Aubert JP, Batra SK. Human MUC4 mucin induces ultra-structural changes and tumorigenicity in pancreatic cancer cells. Brit. J. Cancer 2007;97:345–357. [PubMed: 17595659]
20. Ponnusamy MP, Singh AP, Jain M, Chakraborty S, Moniaux N, Batra SK. MUC4 activates HER2 signalling and enhances the motility of human ovarian cancer cells. Br. J. Cancer 2008;99:520–526. [PubMed: 18665193]
21. Hu YP, Haq B, Carraway KL, Savaraj N, Lampidis TJ. Multidrug resistance correlates with overexpression of Muc4 but inversely with P-glycoprotein and multidrug resistance related protein in transfected human melanoma cells. Biochem. Pharmacol 2003;65:1419–1425. [PubMed: 12732353]
22. Workman HC, Sweeney C, Carraway III KL. The membrane mucin Muc4 inhibits apoptosis induced by multiple insults via ErbB2-dependent and ErbB2-independent mechanisms. Cancer Res 2009;69:2845–2852. [PubMed: 19293191]
23. Leteurtre E, Gouyer V, Rousseau K, Moreau O, Barbat A, Swallow D, Huet G, Lesuffleur T. Differential mucin expression in colon carcinoma HT-29 clones with variable resistance to 5-fluorouracil and methotrexate. Biol. Cell 2004;96:145–151. [PubMed: 15050369]

24. Pino V, Ramsauer VP, Salas P, Carothers Carraway CA, Carraway KL. Membrane mucin Muc4 induces density-dependent changes in ERK activation in mammary epithelial and tumor cells: role in reversal of contact inhibition. J. Biol. Chem 2006;281:29411–29420. [PubMed: 16891313]
25. Funes M, Miller JK, Lai C, Carraway KL III, Sweeney C. The mucin Muc4 potentiates neuregulin signaling by increasing the cell-surface populations of ErbB2 and ErbB3. J. Biol. Chem 2006;281:19310–19319. [PubMed: 16690615]
26. Miyahara N, Shoda J, Ishige K, Kawamoto T, Ueda T, Taki R, Ohkohchi N, Hyodo I, Thomas MB, Krishnamurthy S, Carraway KL, Irimura T. MUC4 interacts with ErbB2 in human gallbladder carcinoma: potential pathobiological implications. Eur. J. Cancer 2008;44:1048–1056. [PubMed: 18397823]
27. Ramsauer VP, Pino V, Farooq A, Carothers Carraway CA, Salas PJ, Carraway KL. Muc4-ErbB2 complex formation and signaling in polarized CACO-2 epithelial cells indicate that Muc4 acts as an unorthodox ligand for ErbB2. Mol. Biol. Cell 2006;17:2931–2941. [PubMed: 16624867]
28. Bafna S, Kaur S, Momi N, Batra SK. Pancreatic cancer cells resistance to gemcitabine: the role of MUC4 mucin. Brit. J. Cancer 2009;101:1155–1161. [PubMed: 19738614]
29. Moniaux N, Varshney GC, Chauhan SC, Copin MC, Jain M, Wittel UA, Andrianifahanana M, Aubert JP, Batra SK. Generation and characterization of anti-MUC4 monoclonal antibodies reactive with normal and cancer cells in humans. J. Histochem. Cytochem 2004;52:253–261. [PubMed: 14729877]
30. Mimeault M, Johansson SL, Venkatraman G, Moore E, Henichart JP, Depreux P, Lin MF, Batra SK. Combined targeting of epidermal growth factor receptor and hedgehog signaling by gefitinib and cyclopamine cooperatively improves the cytotoxic effects of docetaxel on metastatic prostate cancer cells. Mol. Cancer Ther 2007;6:967–978. [PubMed: 17363490]
31. Mimeault M, Venkatraman G, Johansson SL, Moore E, Henichart JP, Depreux P, Lin MF, Batra SK. Novel combination therapy against metastatic and androgen-independent prostate cancer by using gefitinib, tamoxifen and etoposide. Int. J. Cancer 2007;120:160–169. [PubMed: 17013895]
32. Mimeault M, Johansson SL, Henichart JP, Depreux P, Batra SK. Cytotoxic effects induced by docetaxel, gefitinib and cyclopamine on side population and non-side population cell fractions from human tumorigenic and invasive prostate cancer cells. Mol. Cancer Ther 2010;9:617–630. [PubMed: 20179163]
33. Mimeault M, Moore E, Moniaux N, Henichart JP, Depreux P, Lin MF, Batra SK. Cytotoxic effects induced by a combination of cyclopamine and gefitinib, the selective hedgehog and epidermal growth factor receptor signaling inhibitors, in prostate cancer cells. Int. J. Cancer 2006;118:1022–1031. [PubMed: 16108016]
34. Hirst SJ, Barnes PJ, Twort CH. Quantifying proliferation of cultured human and rabbit airway smooth muscle cells in response to serum and platelet-derived growth factor. Am. J. Respir. Cell Mol. Biol 1992;7:574–581. [PubMed: 1449805]
35. Castedo M, Ferri K, Roumier T, Metivier D, Zamzami N, Kroemer G. Quantitation of mitochondrial alterations associated with apoptosis. J. Immunol. Methods 2002;265:39–47. [PubMed: 12072177]
36. Bossy-Wetzel E, Newmeyer DD, Green DR. Mitochondrial cytochrome c release in apoptosis occurs upstream of DEVD-specific caspase activation and independently of mitochondrial transmembrane depolarization. EMBO J 1998;17:37–49. [PubMed: 9427739]
37. Mimeault M, Batra SK. Characterization of non-malignant and malignant prostatic stem/progenitor cells by Hoecsht side population method. Methods Mol. Biol 2009;568:139–149. [PubMed: 19582424]
38. Singh AP, Chauhan SC, Andrianifahanana M, Moniaux N, Meza JL, Copin MC, van Seuningen I, Hollingsworth MA, Aubert JP, Batra SK. MUC4 expression is regulated by cystic fibrosis transmembrane conductance regulator in pancreatic adenocarcinoma cells via transcriptional and post-translational mechanisms. Oncogene 2007;26:30–41. [PubMed: 16799633]
39. Mimeault M, Hauke R, Mehta PP, Batra SK. Recent advances on cancer stem/progenitor cell research: therapeutic implications for overcoming resistance to the most aggressive cancers. J. Mol. Cell. Med 2007;11:981–1011.
40. Hadnagy A, Gaboury L, Beaulieu R, Balicki D. SP analysis may be used to identify cancer stem cell populations. Exp. Cell Res 2006;312:3701–3710. [PubMed: 17046749]

41. Hermann PC, Huber SL, Herrler T, Aicher A, Ellwart JW, Guba M, Bruns CJ, Heeschen C. Distinct populations of cancer stem cells determine tumor growth and metastatic activity in human pancreatic cancer. Cell Stem Cell 2007;1:313–323. [PubMed: 18371365]
42. Hermann PC, Huber SL, Heeschen C. Metastatic cancer stem cells: a new target for anti-cancer therapy? Cell Cycle 2008;7:188–193. [PubMed: 18256530]
43. Price-Schiavi SA, Jepson S, Li P, Arango M, Rudland PS, Yee L, Carraway KL. Rat Muc4 (sialomucin complex) reduces binding of anti-ErbB2 antibodies to tumor cell surfaces, a potential mechanism for herceptin resistance. Int. J. Cancer 2002;99:783–791. [PubMed: 12115478]
44. Nagy P, Friedlander E, Tanner M, Kapanen AI, Carraway KL, Isola J, Jovin TM. Decreased accessibility and lack of activation of ErbB2 in JIMT-1, a herceptin-resistant, MUC4-expressing breast cancer cell line. Cancer Res 2005;65:473–482. [PubMed: 15695389]
45. Komatsu M, Yee L, Carraway KL. Overexpression of sialomucin complex, a rat homologue of MUC4, inhibits tumor killing by lymphokine-activated killer cells. Cancer Res 1999;59:2229–2236. [PubMed: 10232613]
46. Mimeault M, Brand RE, Sasson AA, Batra SK. Recent advances on the molecular mechanisms involved in pancreatic cancer progression and therapies. Pancreas 2005;31:301–316. [PubMed: 16258363]
47. Brand RE, Lerch MM, Rubinstein WS, Neoptolemos JP, Whitcomb DC, Hruban RH, Brentnall TA, Lynch HT, Canto MI. Advances in counselling and surveillance of patients at risk for pancreatic cancer. Gut 2007;56:1460–1469. [PubMed: 17872573]
48. Jemal A, Siegel R, Ward E, Hao Y, Xu J, Murray T, Thun MJ. Cancer statistics. CA Cancer J. Clin 2008;58:71–96. [PubMed: 18287387]
49. Mimeault M, Batra SK. Recent progress on normal and malignant pancreatic stem/progenitor cell research: therapeutic implications for the treatment of type 1 or 2 diabetes mellitus and aggressive pancreatic cancer. Gut 2008;57:1456–1468. [PubMed: 18791122]
50. Rivera F, Lopez-Tarruella S, Vega-Villegas MA, Salcedo M. Treatment of advanced pancreatic cancer: from gemcitabine single agent to combinations and targeted therapy. Cancer Treat. Rev 2009;35:335–339. [PubMed: 19131170]
51. El Maalouf G, Le Tourneau C, Batty GN, Faivre S, Raymond E. Markers involved in resistance to cytotoxics and targeted therapeutics in pancreatic cancer. Cancer Treat. Rev 2009;35:167–174. [PubMed: 19027240]
52. Bai J, Sata N, Nagai H. Gene expression analysis for predicting gemcitabine sensitivity in pancreatic cancer patients. Off. J. Int. Hepato Pancreato Biliary Assoc. HPB (Oxford) 2007;9:150–155.
53. Garcea G, Dennison AR, Pattenden CJ, Neal CP, Sutton CD, Berry DP. Survival following curative resection for pancreatic ductal adenocarcinoma. A systematic review of the literature. J. Pancreas JOP 2008;9:99–132.
54. Jimeno A, Feldmann G, Suarez-Gauthier A, Rasheed Z, Solomon A, Zou GM, Rubio-Viqueira B, Garcia-Garcia E, Lopez-Rios F, Matsui W, Maitra A, Hidalgo M. A direct pancreatic cancer xenograft model as a platform for cancer stem cell therapeutic development. Mol. Cancer Ther 2009;8:310–314. [PubMed: 19174553]
55. Zhou J, Wang CY, Liu T, Wu B, Zhou F, Xiong JX, Wu HS, Tao J, Zhao G, Yang M, Gou SM. Persistence of side population cells with high drug efflux capacity in pancreatic cancer. World J. Gastroenterol 2008;14:925–930. [PubMed: 18240351]

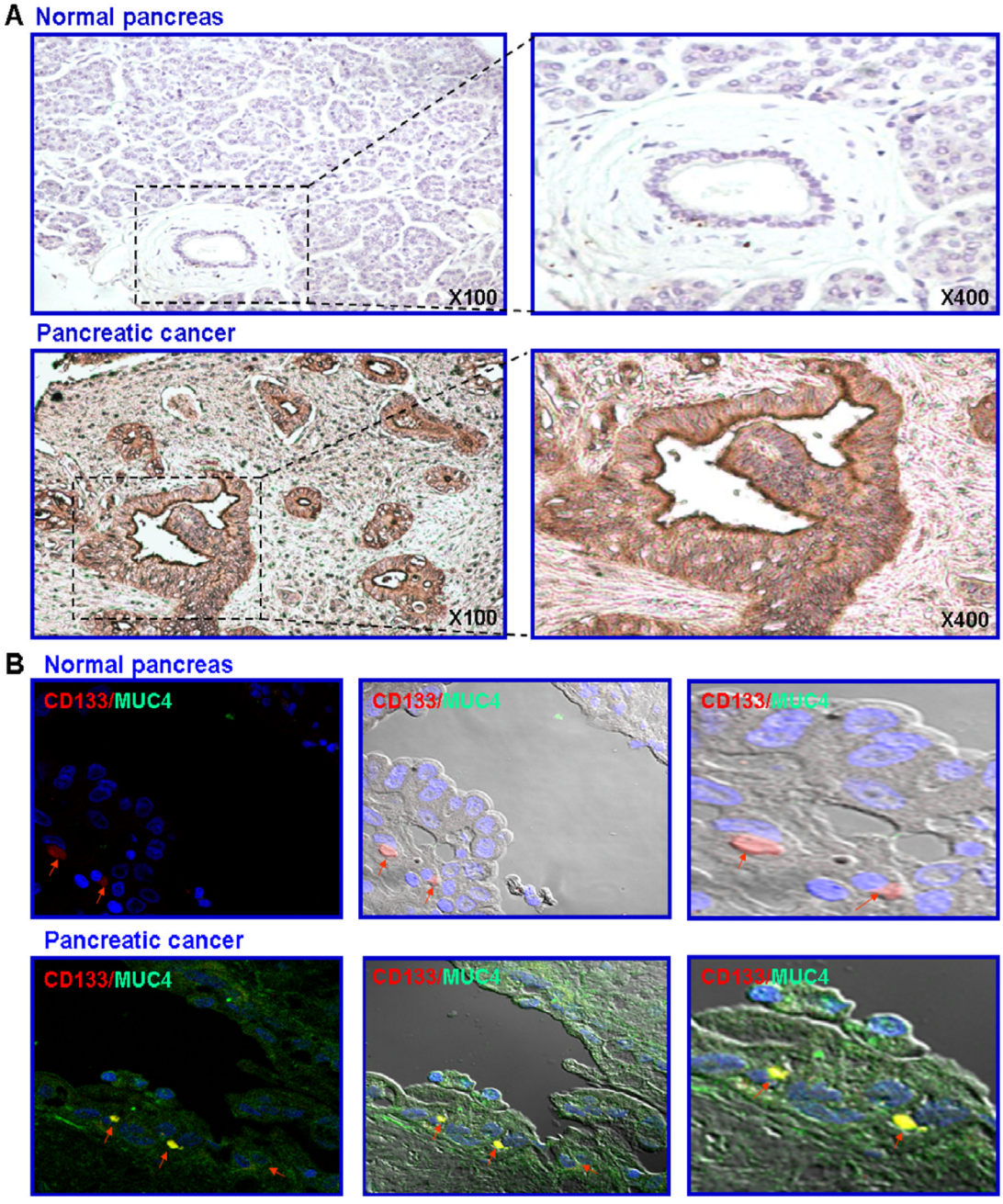

Fig. 1.

Immunohistochemical and immunofluorescence analyses of MUC4 expression level and its co-localization with the CD133 stem cell-like marker in normal and pancreatic adenocarcinoma tissue specimens from patients. (A) Tissue microarray sections of normal and malignant pancreatic tissue samples were probed with anti-MUC4 monoclonal antibody after blocking non-specific staining with horse serum. All sections were examined under a microscope and the immunoreactivity was judged by dark brown staining. Representative pictures of stained tissue samples of normal pancreas and adenocarcinoma obtained are shown at the original magnification of ×100 and ×400. (B) Double-immunofluorescence staining was simultaneously performed with the fluorescein (FITC)-labeled anti-MUC4 primary

monoclonal antibody (green color) and phycoerythrin-labeled anti-CD133 antibody (red color) and nucleus stained with DAPI (blue color), after blocking of non-specific staining with goat serum. Double staining (yellow/purple color) was detected by confocal analyses, which is indicative of the co-localization of these markers, are shown with an arrow. (For interpretation of the references to colour in this figure legend, the reader is referred to the web version of this article.)

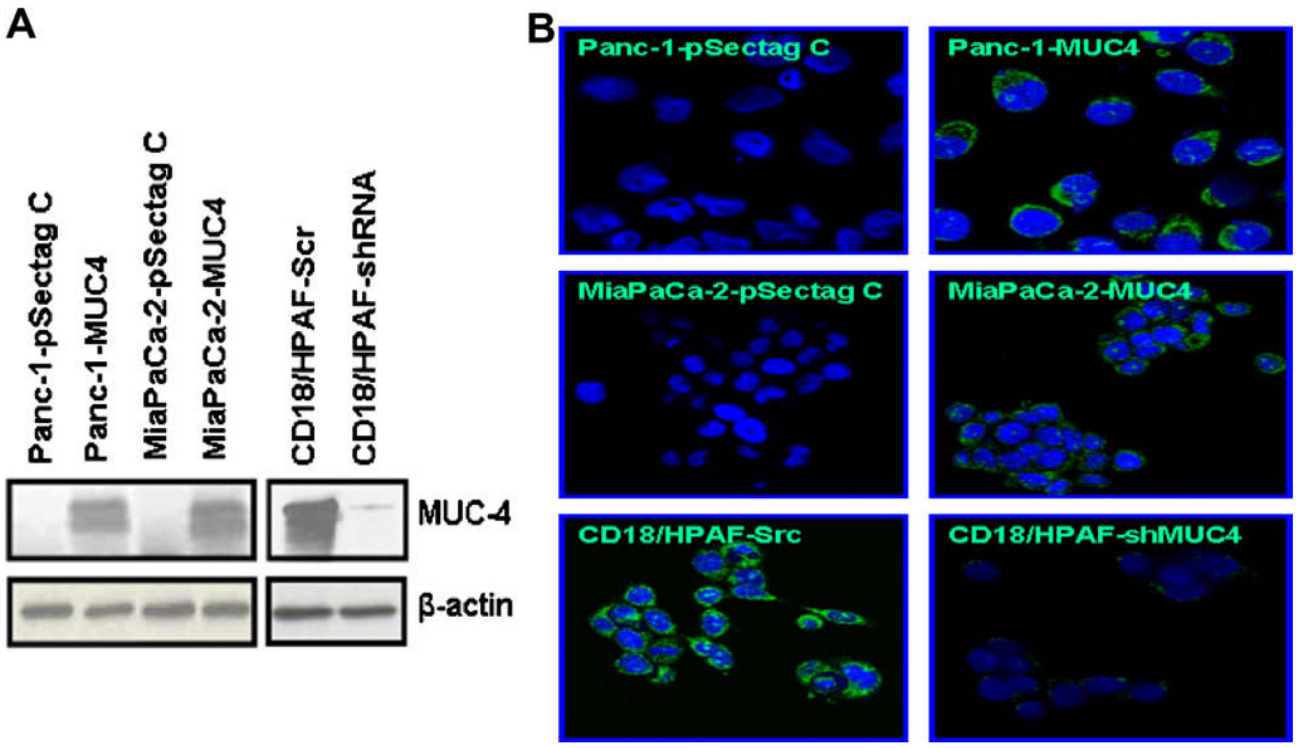

Fig. 2.

Immunoblot and immunofluorescence analyses of MUC4 expression level in established PC cell lines. The stable clones of MUC4 transfected Panc-1 and MiaPaCa-2 cells overexpressing functional MUC4 protein (Panc-1- and MiaPaCa-2-MUC4) and empty-vector transfected Panc-1 and MiaPaCa-2 cell lines (Panc-1- and MiaPaCa-2-pSectag C) as well as the stable clones of MUC4-silenced CD18/HPAF-shMUC4 and empty-vector transfected CD18/HPAF-Src cells expressing endogenous MUC4 were used for these analyses. (A) Western blot analysis was performed with a total of 20 μg proteins from cell lysates. The proteins were resolved on 2% SDS-agarose gel (for MUC4) and 10% SDS-polyacrylamide gel (for β-actin) and immunoblotted with the anti-MUC4 or anti-β-actin monoclonal antibody. The antibody-antigen complexes were visualized using enhanced chemiluminescence technique with horseradish peroxidase-conjugated secondary antibody. (B) Immunoconfocal analyses of the expression level and subcellular localization of the MUC4 oncoprotein in the methanol-fixed PC cells was done with the FITC-conjugated anti-MUC4 antibody (green color) and DAPI (nuclear blue color) after blocking with goat serum. Representative immunofluorescence pictures are shown at the original magnification ×630. (For interpretation of the references to colour in this figure legend, the reader is referred to the web version of this article.)

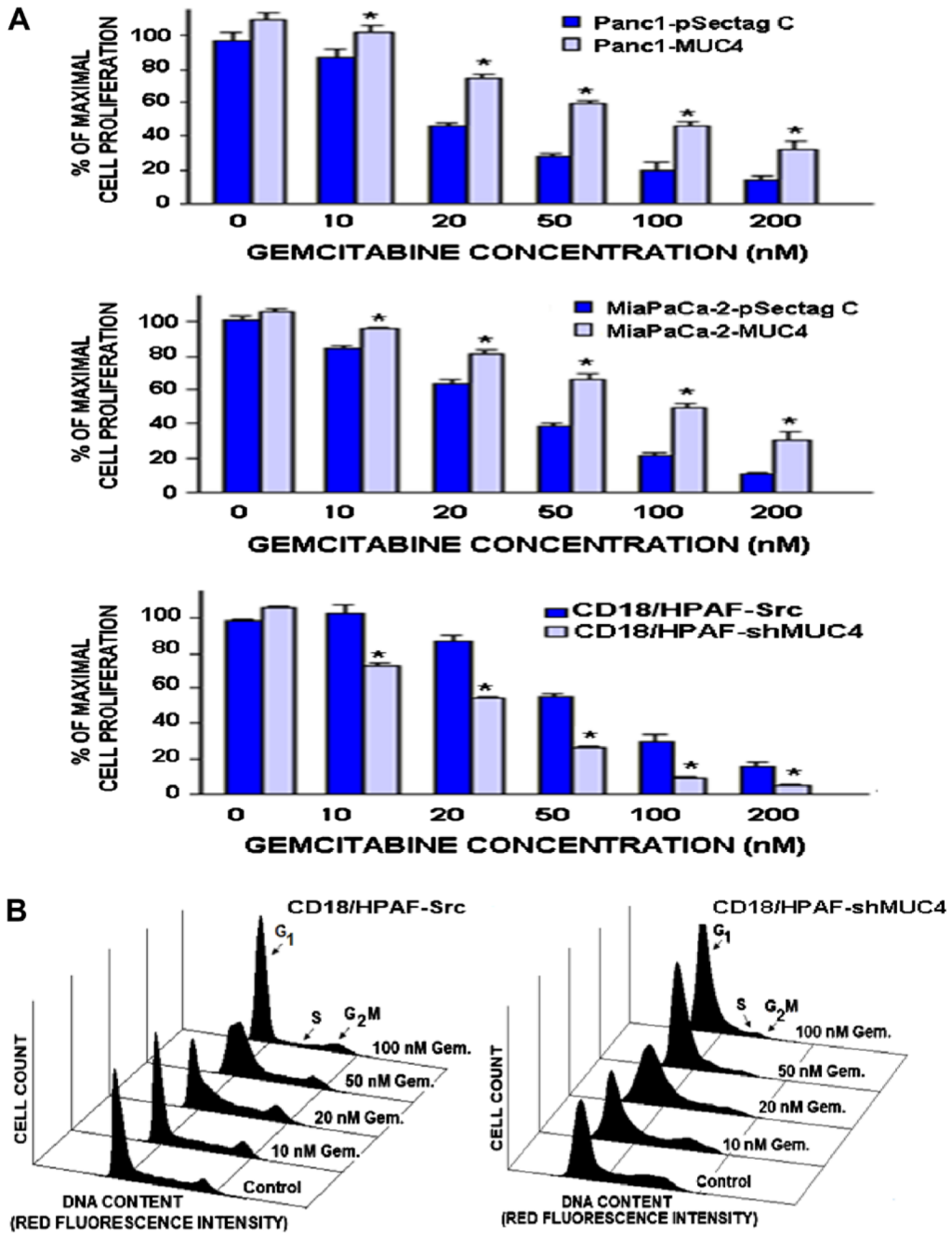

Fig. 3.

Anti-proliferative effects induced by gemcitabine treatment on MUC4 non-expressing- and expressing-PC cell lines. The PC cells were untreated (control) or treated with indicated gemcitabine (Gem.) concentrations for two days. The cell proliferation was evaluated by (A) MTT assays and (B) the analyses of cell cycle phases by FACS for CD18/HPAF-Src and CD18/HPAF-shMUC4 cells. *$p < 0.05$, indicates a significant difference between the anti-proliferative effect induced by gemcitabine treatment on Panc-1- or MiaPaCa-2-MUC4 cells engineered for overexpressing MUC4 protein *versus* empty-vector transfected Panc-1- or MiaPaCa-2-pSectag C cells and MUC4-silenced CD18/HPAF-shMUC4 *versus* scrambled CD18/HPAF-Src cells overexpressing endogenous MUC4.

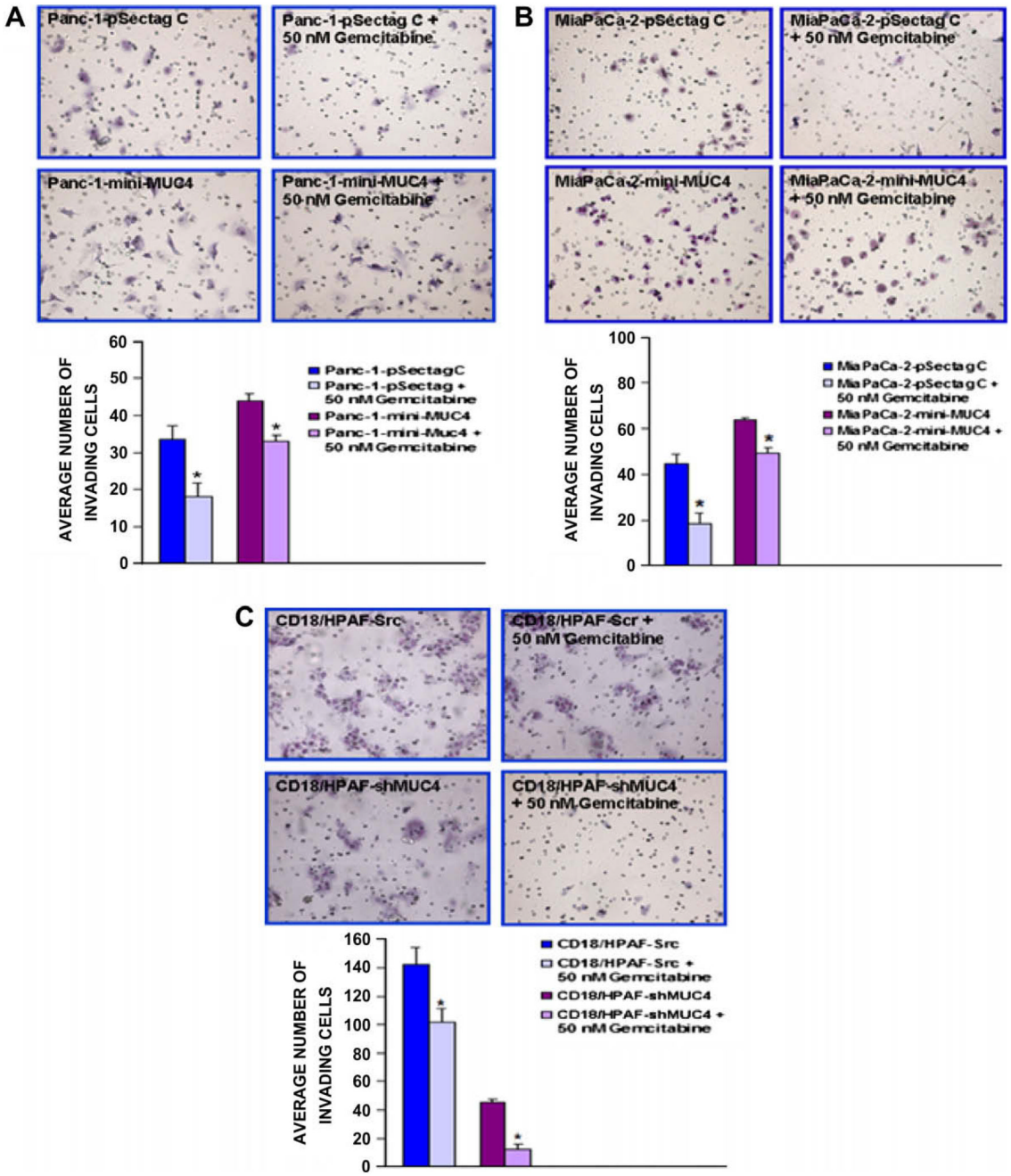

Fig. 4.

Anti-invasive effects of gemcitabine treatment on MUC4 non-expressing and expressing-PC cell lines. The PC cells were plated on matrigel-coated membrane for invasion assays and incubated for 24 h. Data obtained for (A) non-expressing Panc-1-pSectag and Panc-1-MUC4 cells engineered for overexpressing MUC4 protein, (B) non-expressing MiaPaCa-2-pSectag C cells and MiaPaCa-2-MUC4 cells engineered for overexpressing MUC4 protein, and (C) scrambled CD18/HPAF-Src overexpressing endogenous MUC4 and MUC4-silenced CD18/HPAF-shMUC4 cells are presented as the number of cells per field of view. *$p < 0.0001$, indicates a significant difference between the invasive ability of untreated PC cells *versus* PC cells treated with 50 nM gemcitabine.

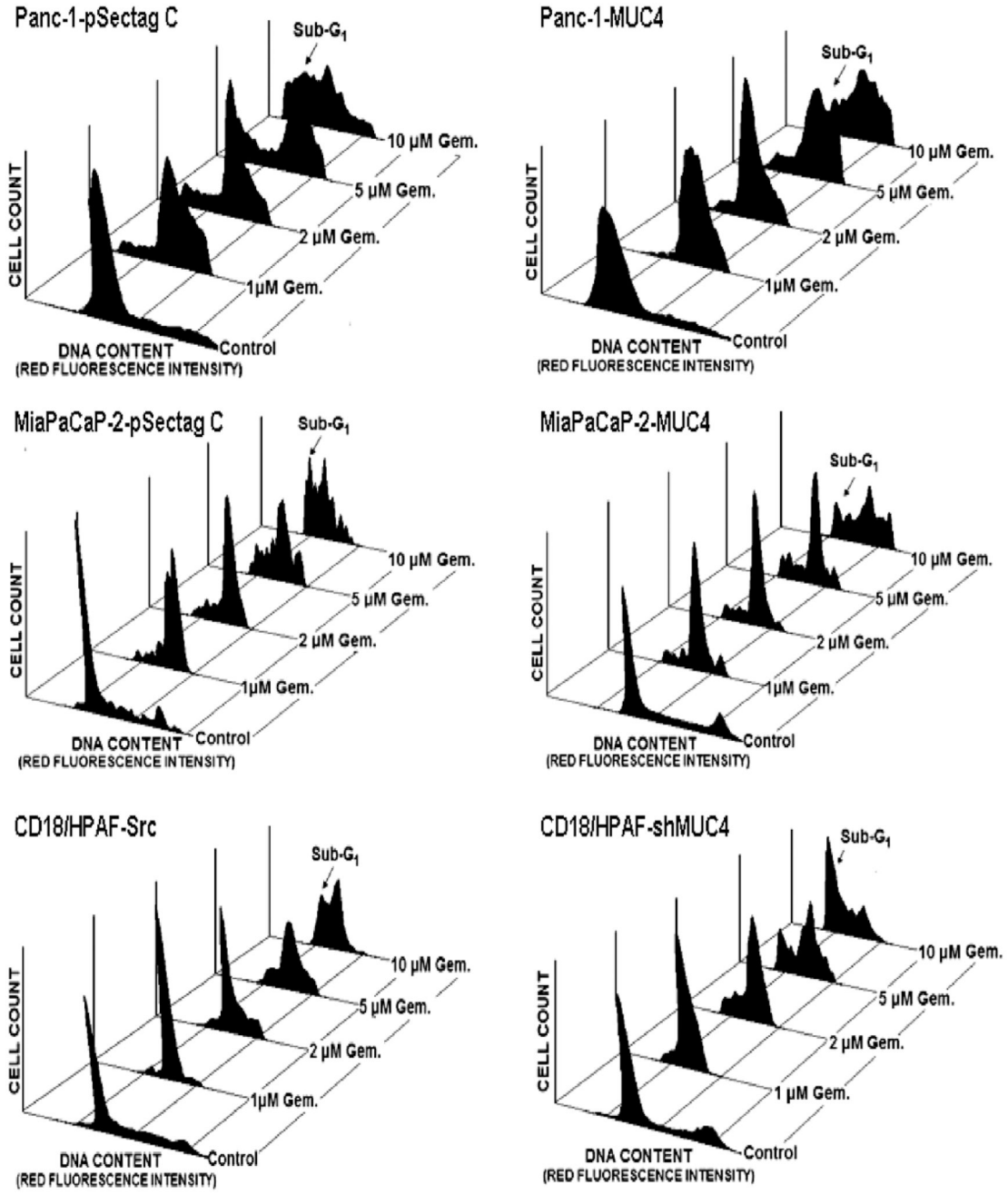

Fig. 5.

FACS analyses of the apoptotic effects induced by gemcitabine treatment on MUC4 non-expressing and overexpressing-PC cell lines. The PC cells were untreated (control) or treated with indicated gemcitabine (Gem.) concentrations for four days. Then, the cell nuclei were stained with propidium iodide and the DNA content was analyzed by flow cytometry.

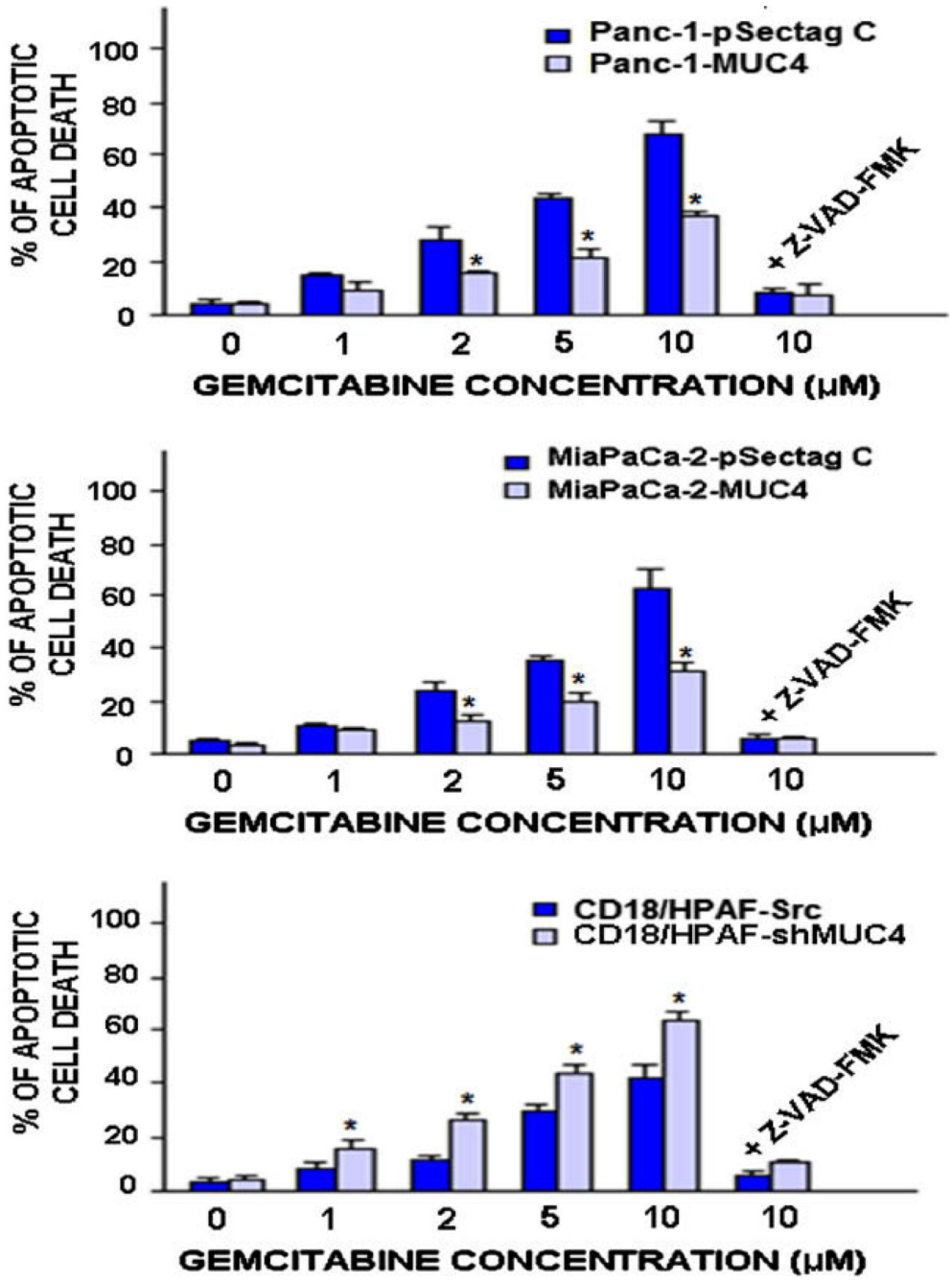

Fig. 6.

Quantification of apoptotic effects induced by gemcitabine treatment on MUC4 non-expressing and overexpressing-PC cell lines. Plots showing the percentages of apoptotic PC cells induced after four days of treatment with indicated gemcitabine (Gem.) concentrations in the absence or presence of broad caspase inhibitor, Z-VAD-FMK, which were estimated by the number of apoptotic cells detected in sub-G1 phase by FACS analyses. *$p < 0.05$, indicates a significant difference between the apoptotic effect induced by gemcitabine treatment on Panc-1- or MiaPaCa-2-MUC4 cells engineered for overexpressing MUC4 protein *versus* MUC4 non-expressing Panc-1- or MiaPaCa-2-pSectag C cells as well as MUC4-silenced

CD18/HPAF-shMUC4 cells *versus* scrambled CD18/HPAF-Src cells overexpressing endogenous MUC4.

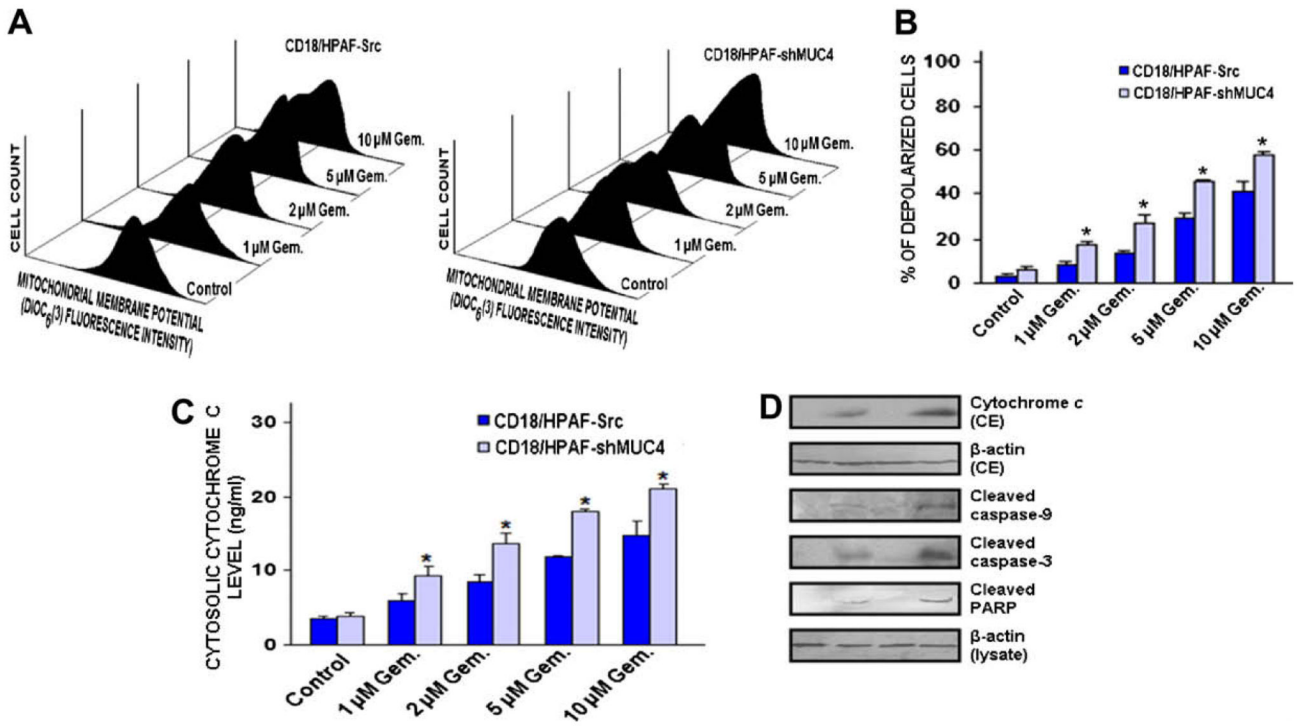

Fig. 7.

Stimulatory effect induced by gemcitabine on mitochondrial membrane potential, cytosolic cytochrome *c* releasing and caspase pathway activation in CD18/HPAF cell lines. The empty-vector transfected CD18/HPAF-Src expressing endogenous MUC4 and MUC4-silenced CD18/HPAF-shMUC4 cells were untreated (control) or treated with indicated concentrations of gemcitabine (Gem.) for four days. After the treatments, the cells were prepared by staining with 40 nM $DIOC_6(3)$ for analyses of mitochondrial membrane potential (MMP) by flow cytometry. Moreover, the amounts of cytochrome *c* released into cytosol were estimated by ELISA as described in Section 2. (A) Representative profiles of stimulatory effect induced by gemcitabine on MMP in the PC cells are shown. (B) Plots showing the percentage of depolarized PC cells induced after treatment with different gemcitabine concentrations. (C) Plots showing the percentages of the stimulatory effect induced by different gemcitabine concentrations on cytosolic cytocrome *c* release in the PC cells. $*p < 0.05$, indicates a significant difference between the stimulatory effect induced by gemcitabine treatment on the percentage of depolarized cells and cytosolic cytochrome *c* amount in CD18/HPAF-shMUC4 *versus* scrambled CD18/HPAF-Src cells expressing MUC4. (D) Western blot analyses of the expression levels of cytosolic cytochrome *c*, cleaved caspases −3 and −9, and cleaved PARP fragment detected in MUC4 silenced CD18/HPAF-shMUC4 *versus* scrambled CD18/ HPAF-Src cells untreated (control) or treated with 10 μM gemcitabine during four days.

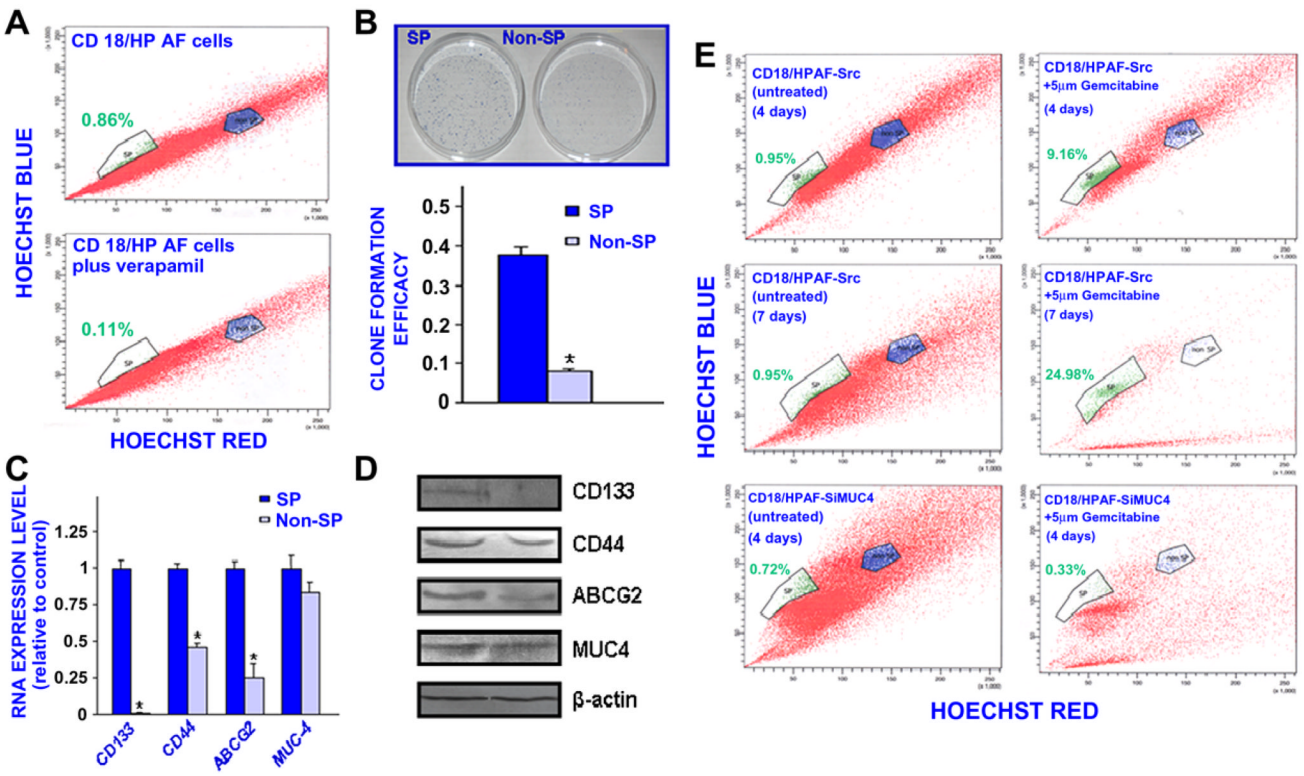

Fig. 8.

Characterization of self-renewal ability and phenotypic features of the SP and non-SP cell fractions isolated from CD18/HPAF cells by Hoechst dye efflux technique and their sensibility to the cytoxix effect induced by gemcitabine treatment. (A) The CD18/HPAF cells were stained with fluorescent Hoechst dye in the absence or presence of 50 μM verapamil and FACS analyses were performed. The Hoechst dye efflux profile shows the side population "SP" (green color), and non-SP fraction (blue color). The number of total PC cells localized in the SP fraction was significantly reduced in the presence of broad ABC transporter inhibitor, verapamil. (B) Clone formation efficacy of SP and non-SP fractions from CD18/HPAF cells corresponds to the ratio of the clone number to the plated cell numbers. (C) Quantitative real-time PCR and (D) Western blot analyses of expression levels of pancreatic stem cell-like markers (CD133, CD44 and ABCG2) and MUC4 in the SP and non-SP cell fractions isolated from CD18/HPAF cell line. The expression of analysed genes was normalized to that of internal control, β-actin. The results are expressed as fold changes detected in the non-SP cell fraction relative to the SP cell used as reference (average ± S.D. of triplicate reactions). *$p < 0.0001$, indicates a significant difference between the clone formation efficacy and expression levels of analysed genes obtained for the non-SP cell fraction as compared to SP cell subpopulation. (E) Estimation by Hoechst dye efflux technique of the percentage of viable SP and non-SP cells detected in the total mass of scrambled CD18/HPAF-Src cells overexpressing endogenous MUC4 and MUC4-silenced CD18/ HPAF-shMUC4 cells untreated or treated with 5 μM gemcitabine during four or seven days. (For interpretation of the references to colour in this figure legend, the reader is referred to the web version of this article.)

Table 1

Immunohistochemical analyses of the MUC4 expression levels in non-malignant and malignant pancreatic tissue specimens from patients.

Pathology diagnosis	Grade[a]	TNM[b]	MUC4 histoimmunostaining[c]
Normal pancreatic tissue	-	-	10 Negative staining
			0 Positive staining
Pancreatic mucinous adenocarcinoma	1	T2N0M0	0 Negative staining
			1 Positive staining
Pancreatic duct adenocarcinoma	1	T2N1M0	0 Negative staining
			1 Positive staining
Pancreatic mucinous adenocarcinoma	1	T4N0M0	0 Negative staining
			1 Positive staining
Pancreatic duct adenocarcinoma	2	T1NxM0	0 Negative staining
			1 Positive staining
Pancreatic duct adenocarcinoma	2	T1N0M0	0 Negative staining
			1 Positive staining
Pancreatic duct adenocarcinoma	2	T2N0M0	4 Negative staining
			14 Positive staining
Pancreatic duct adenocarcinoma	2	T2N1M0	0 Negative staining
			2 Positive staining
Pancreatic duct adenocarcinoma	2	T3N0M0	1 Negative staining
			12 Positive staining
Pancreatic duct adenocarcinoma	2	T3N0M1	0 Negative staining
			2 Positive staining
Pancreatic duct adenocarcinoma	2	T3N1bM0	0 Negative staining
			1 Positive staining
Pancreatic duct adenocarcinoma	2	T4N0M1	0 Negative staining
			1 Positive staining
Pancreatic duct adenocarcinoma	2–3	T2N0M0	0 Negative staining
			1 Positive staining
Pancreatic duct adenocarcinoma	3	T1N0M0	0 Negative staining
			1 Positive staining
Pancreatic duct adenocarcinoma	3	T2N0M0	3 Negative staining
			5 Positive staining
Pancreatic duct adenocarcinoma	3	T3N0M0	1 Negative staining
			6 Positive staining
Pancreatic duct adenocarcinoma with necrosis	3	T4N1M1	1 Negative staining
			0 Positive staining
Pancreatic duct adenocarcinoma	-	T2N0M0	1 Negative staining
			2 Positive staining
	-	T3N0M0	1 Negative staining
			2 Positive staining

[a]The grade 1–4 in pathology diagnosis is equivalent to grade 1: well-differentiated, grade 2: moderately differentiated, grade 3: poorly differentiated and grade 4: undifferentiated.

[b]TNM grading refers to T: primary tumor (Tx, primary tumor cannot bee assessed; T0, no evidence of primary tumor; T1, tumor invades submucosa; T2, tumor invades muscularis propria; T3, tumor invades through muscularis propria into subserosa or into non-peritonealized pericolic or perirectal tissues; 4, tumor directly invades other organs or structures and/or perforate visceral peritoneum), N: regional lymph nodes (Nx, regional lymph nodes cannot be assessed; N0, No regional lymph node metastasis; N1, metastasis in 1–3 regional lymph nodes; N2, metastasis in 4 or more regional lymph nodes) and M: distant metastases (Mx, distant metastasis cannot be assessed; M0, no distant metastasis; M1, distant metastasis).

[c]Results from MUC4 histoimmunostaining analyses performed with anti-MUC4 monoclonal antibody on tissue microarray sections.

Table 2

Inhibitory effect induced by gemcitabine treatment on the cell cycle progression of pancreatic cancer cells.

Cell type/tested agent	Cell population in cell cycle phases (%)[a]		
	[b]G1/early S	S	G_2/M
CD18/HPAF-Src			
0 nM Gemcitabine	61.3 ± 1.7	26.4 ± 2.4	12.3 ± 0.8
10 nM Gemcitabine	63.6 ± 0.5	26.0 ± 0.2	10.7 ± 0.7
20 nM Gemcitabine	68.1 ±1.2	21.4 ± 1.3	10.5 ± 0.2
50 nM Gemcitabine	74.4 ±0.7	15.9 ± 0.3	10.7 ± 0.3
100 nM Gemciabine	82.4 ± 0.6	8.4 ± 0.2	9.2 ± 0.4
CD18/HPAF-shMUC4			
0 nM Gemcitabine	66.1 ± 0.7	19.3 ± 0.4	14.6 ± 0.4
10 nM Gemcitabine	74.7 ±1.1	15.5 ± 0.3	9.8 ± 1.2
20 nM Gemcitabine	83.2 ±1.8	11.6 ± 0.5	5.1 ± 0.3
50 nM Gemcitabine	85.5 ±1.8	7.9 ± 0.7	6.6 ± 2.0
100 nM Gemciabine	91.8 ± 0.8	4.8 ± 0.8	3.4 ± 0.1

[a]Data represent the percentage of cells in cell cycle phases observed after 2 days of treatment with indicated gemcitabine concentrations as estimated by the cell counts following FACS analyses. Data are means ± S.E. of 3–6 different experiments.